CASL-U-2019-1847-000

ATF Benchmark Problems

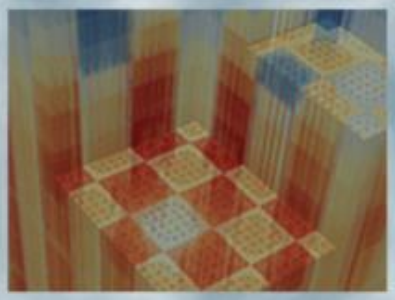

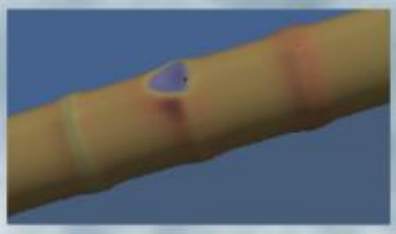

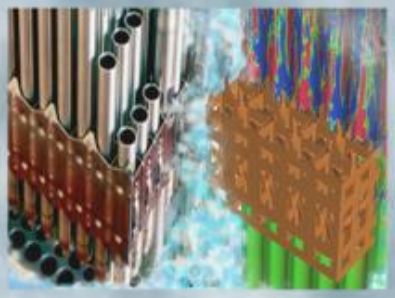

Eva Davidson, ORNL
Fausto Franceschini, Westinghouse
Kang Seog Kim, ORNL

April 30, 2019

DOCUMENT AVAILABILITY

Reports produced after January 1, 1996, are generally available free via US Department of Energy (DOE) SciTech Connect.

Website www.osti.gov

Reports produced before January 1, 1996, may be purchased by members of the public from the following source:

National Technical Information Service
5285 Port Royal Road
Springfield, VA 22161
Telephone 703-605-6000 (1-800-553-6847)
TDD 703-487-4639
Fax 703-605-6900
E-mail info@ntis.gov
Website http://classic.ntis.gov/

Reports are available to DOE employees, DOE contractors, Energy Technology Data Exchange representatives, and International Nuclear Information System representatives from the following source:

Office of Scientific and Technical Information
PO Box 62
Oak Ridge, TN 37831
Telephone 865-576-8401
Fax 865-576-5728
E-mail reports@osti.gov
Website http://www.osti.gov/contact.html

REVISION LOG

Revision	Date	Affected Pages	Revision Description
0	04/30/2019	All	Initial Release

Document pages that are:

Unlimited_____All_____

Export Controlled _____None_____

IP/Proprietary/NDA Controlled__None_____

Sensitive Controlled__None_____

Requested Distribution:

To: N/A

Copy: N/A

EXECUTIVE SUMMARY

In fiscal year 2018, the US Nuclear Regulatory Commission (NRC) expressed an interest in using the US Department of Energy (DOE) Office of Nuclear Energy (NE) advanced modeling and simulation tools to evaluate advanced fuel concepts such as accident-tolerant fuel (ATF). This interest evolved into formal cooperation between DOE and NRC to ensure that advanced modeling and simulation (M&S) capability is available to the NRC for the analyses of ATF concepts. The Consortium for Advanced Simulation of Light Water Reactors (CASL) has developed, applied, and deployed advanced modeling and simulation capabilities to enhance the operational performance, efficiency, and safety of light water reactors (LWRs). As a result of this cooperative effort between DOE and NRC, potential ATF concepts of interest to the industry were identified and simulated with CASL's Virtual Environment for Reactor Applications (VERA) for 2D pressurized water reactor (PWR) 17 × 17 lattices. Four ATF concepts were identified by CASL's Westinghouse collaborators, and the benchmark specifications for these ATF concepts were generated as presented in this report. These benchmark problems were set up to test the ability of VERA to simulate these ATF concepts, and the results generated by VERA were compared against two Monte Carlo codes: (1) Serpent, which was developed at VTT Technical Research Centre of Finland Ltd, and (2) Shift, which was developed at Oak Ridge National Laboratory (ORNL). The depletion parameters and flags used to run these models differ between all three codes, and there were differences seen between VERA, Shift, and Serpent, but overall, the agreement shown was considered sufficient to progress to core modeling and evaluation of these ATF concepts using VERA. The differences identified in this document require further investigation by modeling single fuel pin depletion to compare the isotopic evolution of the fuel during a depletion calculation. Prior depletion benchmarking efforts between VERA and Shift have shown closer agreement for UO_2, so recent changes to the code and the data should be investigated to identify the cause of these differences.

CONTENTS

FIGURES

TABLES

ACRONYMS and ABBREVIATIONS

2D	two-dimensional
ATF	accident-tolerant fuel
ATR	Advanced Test Reactor
BeO	beryllium oxide
Cr	chromium
CASL	Consortium for Advanced Simulation of Light Water Reactors
CE	continuous-energy (cross sections)
CTF	COBRA-TF
DOE	US Department of Energy
FY	fiscal year
GWd/MTU	gigawatt-days per metric ton of uranium
HPC	high-performance computer
INL	Idaho National Laboratory
LFR	lead fuel rod
LTA	lead test assembly
LWR	light-water reactor
M&S	modeling and simulation
NRC	US Nuclear Regulatory Commission
NSSS	nuclear steam supply system
ORNL	Oak Ridge National Laboratory
PWR	pressurized water reactor
T/H	thermal hydraulics
UB_2	uranium boride
$U^{15}N$	uranium nitride
UO_2	uranium dioxide
U_3Si_2	uranium silicide
VERA	Virtual Environment for Reactor Applications

1. INTRODUCTION

The events at Fukushima Daiichi Nuclear Power Plant on March 2011 propelled the research and development of accident-tolerant fuel (ATF) for use in nuclear power plants. After these events, the United States Senate Appropriations Committee requested a report from the United States Department of Energy (DOE) regarding DOE's plan for developing ATF. In DOE's development plan [1], a 10-year effort beginning in 2012 was outlined from Phase 1 feasibility studies through Phase 3 commercialization with a lead test assembly (LTA) or a lead fuel rod (LFR) to be ready for insertion into a reactor by 2022.

In fiscal year 2018, the US Nuclear Regulatory Commission (NRC) expressed an interest in using the DOE Office of Nuclear Energy (NE) advanced modeling and simulation (M&S) tools to evaluate advanced fuel concepts such as ATF. This interest evolved into a formal cooperation between DOE and NRC to ensure that an effective M&S capability is available for NRC analyses of ATF concepts [2].

Over the last 10 years, the DOE-funded Energy Innovation Hub, also known as the Consortium for Advanced Simulation of Light Water Reactors (CASL), has developed, applied and deployed advanced M&S capabilities to enhance the operational performance, efficiency, and safety of light water reactors (LWRs). Due to the aging US nuclear fleet, CASL was initiated to improve the efficiency of nuclear power production, lower costs by enhancing the understanding of fuel performance and residence time in the nuclear reactor, enhance safety by studying new fuels that can endure severe conditions, and extend the life of existing reactors by predicting the lifetimes of key structural components [3].

As a result of the cooperation between DOE and NRC, potential ATF concepts of interest to the industry were identified and simulated with CASL's Virtual Environment for Reactor Applications (VERA) [4] for 2D pressurized water reactor (PWR) 17 × 17 lattices. Four ATF concepts were identified by CASL's Westinghouse collaborators, and benchmark problems were generated as presented in this report. These benchmark problems were set up to test the ability of VERA to simulate these ATF concepts, and the results generated by VERA were compared against two Monte Carlo codes: (1) Serpent [5], developed by the VTT Technical Research Centre of Finland Ltd, and Shift [6], which was developed at Oak Ridge National Laboratory (ORNL).

2. ATF CONCEPTS

Several varieties of ATF concepts are under development in the nuclear industry and in academia. The three main nuclear fuel vendors in the US—Framatome, General Electric (GE) and Westinghouse—are all developing ATF concepts in close research and development partnership with DOE-NE. In January 2019, DOE-NE awarded $111 million in funding through fiscal year 2021 to these three US fuel vendors to develop ATF [7]. The primary objectives of the DOE awards are detailed below [7]:

- GE will continue (1) development of iron chromium aluminum (FeCrAl) alloys cladding, (2) the development of its coating program for zirconium alloys, ARMOR, and (3) the study of uranium dioxide–based ceramic metal fuels;
- Framatome to continue (1) the development and deployment of chromium-coated zirconium alloy cladding with chromia-doped uranium oxide pellets (Cr-Cr_2O_3) and (2) expand development efforts on silicon carbide cladding concepts; and
- Westinghouse to continue the development of uranium silicide and doped uranium oxide fuel, also known as *ADOPT fuel*, in chromium-coated zirconium alloy cladding, and (2) the development of silicon carbide cladding concepts.

For the first 14-month period of the award, the fuel vendors are required to [7] accomplish the following:

- Ensure that an initial LTA has been installed in a US commercial power plant
- Ensure that prototypic pin segments have been installed in the Idaho National Laboratory (INL) Advanced Test Reactor (ATR) water loop;
- Continue development of licensing approaches for the ATF concept, including the involvement of at least one nuclear power plant owner/operator per ATF concept
- Ensure interaction with the NRC for licensing of each concept

Figure 1 [8] shows key ATF testing milestones for the three US fuel vendors. LTAs are expected to be inserted by Framatome in Southern's Vogtle, GE in Exelon's Clinton, and Westinghouse in Exelon's Byron.

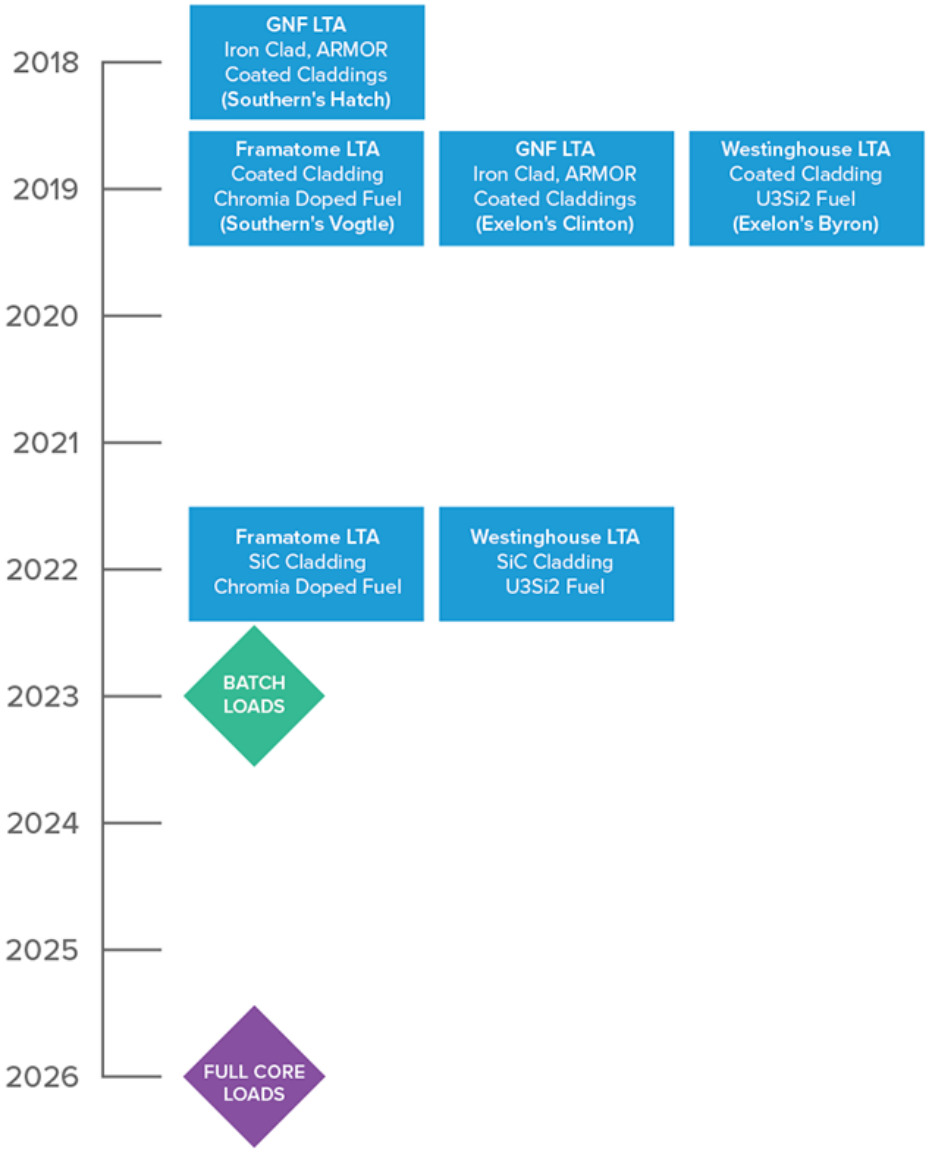

Figure 1. Key ATF testing milestones [8].

To facilitate the licensing of these ATF concepts, it is crucial for DOE-NE to cooperate with the NRC through CASL to identify any modeling and simulation gaps of ATF concepts. The advanced modeling and simulation capabilities developed within CASL can accelerate the design and testing of these advanced fuel concepts. The purpose of this document is to ensure that any modeling and simulation gaps for ATF in VERA are identified and that a set of benchmark problems are prescribed for testing the M&S codes identified within this document. As these codes evolve and are updated, this document may be amended with revised results from the codes identified.

In developing this document, CASL's Westinghouse collaborators identified the following ATF concepts for PWRs as benchmark problems for M&S tools:

- Uranium silicide (U_3Si_2) and beryllium oxide (BeO) fuel and chromium coated ZIRLO® cladding;
- U_3Si_2 with BeO doped with uranium boride (UB_2) and chromium-coated ZIRLO cladding;
- Uranium nitride ($U^{15}N$) with BeO and chromium-coated ZIRLO cladding;
- $U^{15}N$ with BeO doped with UB_2 and chromium-coated ZIRLO cladding

These concepts were developed by Westinghouse to enhance accident tolerance, to simplify designs for future nuclear steam supply systems (NSSSs), and to improve fuel costs, thereby incentivizing their use for utilities [9,10]. Currently, Westinghouse is developing U_3Si_2 pellets as its mid-term fuel product, whereas the waterproofed $U^{15}N$ fuel is being considered as the long-term fuel product [9,10]. The chromium coating on zirconium cladding is expected to reduce oxidation and hydriding and to provide an improvement in temperature tolerance in severe accident scenarios. U_3Si_2 fuel provides a 17% increase in ^{235}U and an increase in thermal conductivity by a factor of 2–5 as compared to UO_2 [9,10]. $U^{15}N$ [9,10] fuel provides an increase in ^{235}U of ~35% and an increase in thermal conductivity by factor of 5–10 [9,10]. Westinghouse is currently partnering with INL, Los Alamos National Laboratory (LANL), Texas A&M University, and National Nuclear Laboratory (NNL) in the United Kingdom for the development and fabrication of waterproofed U_3Si_2 and $U^{15}N$ fuel concepts [10]. The addition of BeO to U_3Si_2 and UN is intended to simulate addition of a fuel dopant, and the addition of U dilutant will improve the high-temperature water resistance of these ATF concepts. ADOPT was not specifically benchmarked in this study due to its obvious similarity to UO_2 fuel. Therefore, besides adding ADOPT to the related modeling capability in VERA, no specific benchmarking exercise has been devised for this option, as it is deemed to be already covered by the extensive benchmarking activities performed for UO_2 fuel. The results from these ATF concept analyses are compared against UO_2 results for a 17 × 17 Westinghouse PWR assembly.

3. CODES

M&S tools used to simulate these benchmark problems were VERA, Serpent, and Shift. CASL's VERA offers unique capabilities that combine high-fidelity in-core and ex-core radiation transport. Figure 2 shows an overview of VERA, which is composed of multiple physics components for reactor simulation and direct coupling between these physics. A lot of attention is given to the usability of VERA and its parallel performance on high performance computer systems (HPCs). VERA's deterministic neutronics code MPACT [11] performs in-core radiation transport with temperature feedback using COBRA-TF (CTF) [12]. MPACT performs a direct whole-core 3D neutron transport calculation with 51 energy groups, explicit pin-by-pin powers with intra-pin distributions, explicit pin-by-pin depletion and decay at local conditions, and semi-explicit 3D reflector geometry. In addition to performing the neutron transport calculation, local thermal-hydraulic (T/H) conditions for feedback are calculated using CTF with fuel temperatures for each

rod, as well as sub-channel T/H with transient two-fluid, three-field (liquid film, liquid drops and vapor) solutions in coolant channels with cross-flow. ORIGEN [13] is used to perform isotopic depletion and decay, with 263 isotopes being tracked. MPACT can also perform a critical boron search, control rod movements, fuel shuffling, and in-core instrumentation response, as well as read and write restart files at various state points.

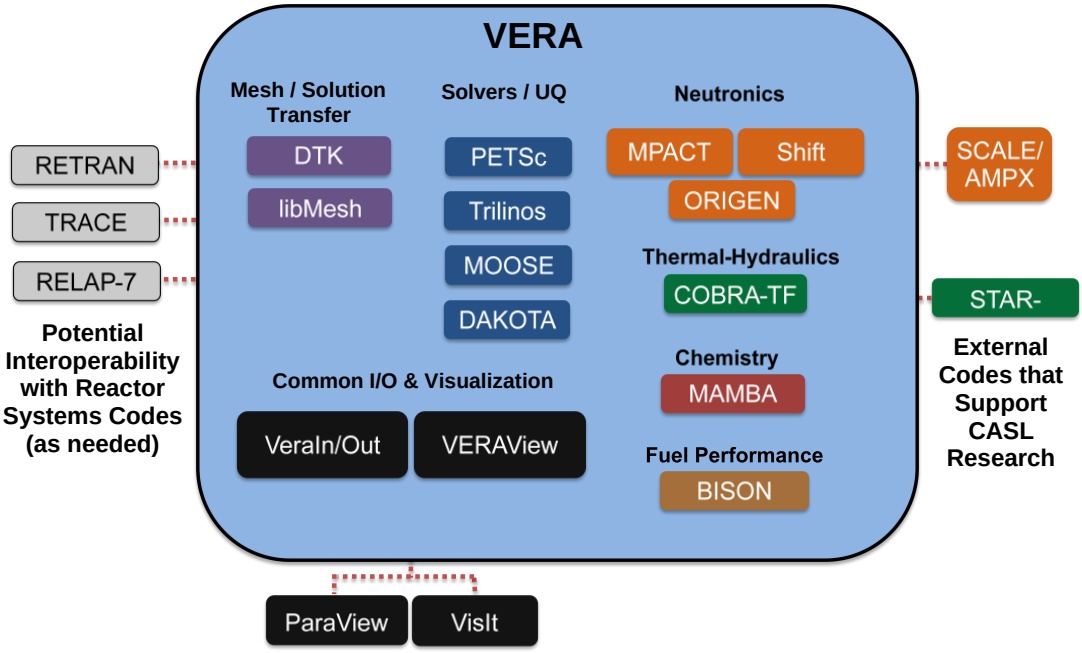

Figure 2. Virtual Environment for Reactor Applications (VERA).

The Shift Monte Carlo code is developed at ORNL and it is part of the Exnihilo code suite. It is a flexible, high-performance Monte Carlo radiation transport framework designed to scale from supercomputers to laptops. It has multiple front ends through the following:

1. Omnibus: fully featured general front-end
2. SCALE [14]: integrated into CSAS, TRITON and MAVRIC,
3. Insilico: integrated into VERA for in-core and ex-core analyses.

Shift is a physics-agnostic code, which means that it can run continuous energy (CE) or multigroup physics engines with SCALE. Shift is also geometry agnostic and has the ability to run on any of the following geometries through its Omnibus front end: Exnihilo RTK, MCNP [15], GG (KENO/SCALE), DAGMC CAD. Shift has fixed source and eigenvalue solvers. Research and development into state-of-the-art methods and algorithms has been performed and implemented within Shift. Shift is also capable of performing hybrid Monte Carlo / deterministic calculations for efficient calculations of deep penetration problems, and it can perform Monte Carlo depletion calculations. More recently, GPU implementation for CE physics with reactor geometry has been demonstrated with Shift.

The Serpent Monte Carlo code is developed by VTT Technical Research Centre of Finland, Ltd. It is a multipurpose 3D CE Monte Carlo code, and it can be run in parallel on HPCs. The applications for Serpent are divided into three categories [16]:

1. Reactor physics applications: spatial homogenization, criticality calculations, fuel cycle studies, research reactor modeling, and validation of deterministic transport codes

2. Multi-physics simulations: coupled calculations with thermal hydraulics, CFD and fuel performance codes
3. Neutron and photon transport simulations for radiation dose rate calculations, shielding, fusion research and medical physics

Serpent uses surface tracking and Woodcock delta-tracking methods for particle transport, and it reads CE cross sections from ACE format libraries. Serpent can simulate explicit particle and pebble-bed fuel models for HTGR calculations. Serpent can import CAD and unstructured mesh-based geometries. Serpent can also perform Monte Carlo depletion calculations, and two-way coupling to thermal-hydraulics, CFD, and fuel performance codes.

4. INPUT PARAMETERS

The inputs used in all the codes were kept consistent to enable consistency in the code-to-code comparisons and benchmarking. This section covers the geometry, materials, temperature, specific power, and densities used to set up the models for VERA, Shift, and Serpent.

4.1. GEOMETRY AND DEPLETABLE REGIONS

A 2D 17 × 17 PWR assembly was set up for all three codes. An MCNP model was set up to perform the Shift calculation. As mentioned earlier, Shift is geometry agnostic, and it can read MCNP geometry and perform Shift-based physics and depletion calculations with SCALE data using the MCNP geometry input format. The VERA, Serpent, and Shift models were set up consistently using the radii and pitch prescribed in Table 1 [17, 18]. In all the three codes, each fuel pin is subdivided into three depletable regions of equal volumes, and the depleted isotopes are tracked within each of these cells. The radii of each of these subdivided depletable fuel regions are shown in Table 2. There are 264 fuel pins which subsequently result in 792 depletable fuel regions that must be tracked. Figure 3 shows the depletable fuel regions in each pin cell marked with a red-hued cylinder, which is surrounded by ZIRLO clad in UO_2 and an additional chromium coating for U_3Si_2-BeO, U_3Si_2-BeO-UB_2, $U^{15}N$-BeO, and $U^{15}N$-BeO-UB_2 models. The fuel pin, lattice and assembly pitch dimensions, the guide tube dimensions, and the UO_2 fuel and ZIRLO clad radii can be found in [17] and are presented here. The ATF fuel pin, ZIRLO clad and Cr coating dimensions are Westinghouse-approved dimensions for release obtained during this work [18].

Table 1. Geometry input parameters [17, 18]

PWR 17 × 17 geometry parameters (cm)	UO_2	U_3Si_2-BeO	U_3Si_2-BeO-UB_2	$U^{15}N$-BeO	$U^{15}N$-BeO-UB_2
Fuel radius	0.409575	0.403860	0.403860	0.382333	0.382333
ZIRLO clad outer radius	0.474980	0.468884	0.468884	0.447358	0.447358
Cr coating outer radius	-	0.471384	0.471384	0.449858	0.449858
Fuel pin pitch	1.25984	1.25984	1.25984	1.25984	1.25984
Guide tube inner radius	0.56134	0.56134	0.56134	0.56134	0.56134
Guide tube outer radius	0.601984	0.601984	0.601984	0.601984	0.601984
Lattice pitch	21.41728	21.41728	21.41728	21.41728	21.41728
Assembly pitch	21.50364	21.50364	21.50364	21.50364	21.50364

Table 2. Radii of depletable regions

PWR 17 × 17 geometry parameters (cm)	UO_2	U_3Si_2-BeO	U_3Si_2-BeO-UB_2	$U^{15}N$-BeO	$U^{15}N$-BeO-UB_2
Fuel ring 1 radius	0.236468	0.233169	0.233169	0.220740	0.220740
Fuel ring 2 radius	0.334417	0.329750	0.329750	0.312174	0.312174
Fuel ring 3 radius	0.409575	0.403860	0.403860	0.382333	0.382333

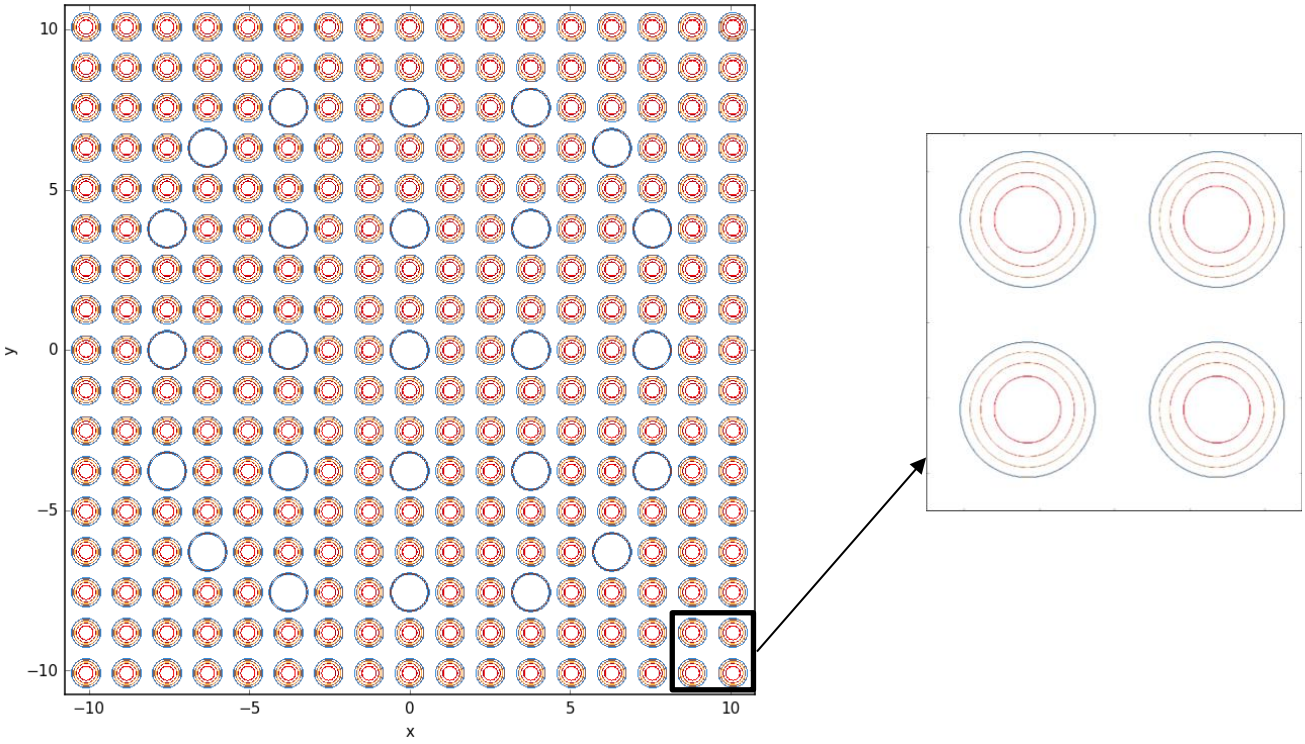

Figure 3. PWR lattice with three depletable fuel regions (zoomed in view of 2x2 pins).

4.2. MATERIAL

The fuel material in each depletable region for five fuel types at the first time-step (zero burnup) is defined in Table 3. Table 4 shows non-fuel material compositions that are common to all the models: ZIRLO clad, Cr coating (if applicable), moderator, and ZIRLO guide tube.

Table 3. Fuel material compositions [17, 18]

Fuel	Isotope	Number density (atoms/b-cm)
UO_2	92234	1.0908303E-05
	92235	1.1490359E-03
	92236	3.3607102E-07
	92238	2.1774061E-02
	8016	4.5868683E-02
U_3Si_2-BeO	92234	1.2333554E-05
	92235	1.2991660E-03
	92236	3.7998120E-07
	92238	2.4619004E-02
	8016	3.4496489E-03
	14028	1.5913068E-02
	14029	8.0839619E-04
	14030	5.3352423E-04
	4009	3.4496489E-03
U_3Si_2-BeO-UB_2	92234	1.2334648E-05
	92235	1.2992813E-03
	92236	3.8001492E-07
	92238	2.4621189E-02
	8016	3.4499025E-03
	14028	1.5913068E-02
	14029	8.0839619E-04
	14030	5.3352423E-04
	4009	3.4499025E-03
	5010	1.0140637E-04
$U^{15}N$-BeO	92234	1.4644320E-05
	92235	1.5425727E-03
	92236	4.5117299E-07
	92238	2.9231524E-02
	8016	3.6535150E-03
	7014	3.0789193E-04
	7015	3.0481301E-02
	4009	3.6535150E-03
$U^{15}N$-BeO-UB_2	92234	1.4640966E-05
	92235	1.5422193E-03
	92236	4.5106965E-07
	92238	2.9224829E-02
	8016	3.6527297E-03
	7014	3.0728433E-04
	7015	3.0421149E-02
	4009	3.6527297E-03
	5010	1.0741552E-04

Table 4. Non-fuel material compositions

Common materials	Isotope	Number density (atoms/b-cm)
ZIRLO clad	8016	2.7100759E-04
	26054	3.9934579E-06
	26056	6.2688768E-05
	26057	1.4477573E-06
	26058	1.9267001E-07
	40090	1.9125365E-02
	40091	4.1893667E-03
	40092	6.3825560E-03
	40094	6.4420329E-03
	40096	1.0334030E-03
	41093	3.7336177E-04
	50112	2.8344530E-06
	50114	1.9286143E-06
	50115	9.9349173E-07
	50116	4.2486366E-05
	50117	2.2441250E-05
	50118	7.0771782E-05
	50119	2.5100285E-05
	50120	9.5199920E-05
	50122	1.3529034E-05
	50124	1.6918603E-05
Chromium coating	24050	3.5980710E-03
	24052	6.9385218E-02
	24053	7.8677267E-03
	24054	1.9584437E-03
Moderator	1001	4.7312447E-02
	8016	2.3659884E-02
ZIRLO guide tube	8016	3.0728566E-04
	26054	4.5280367E-06
	26056	7.1080515E-05
	26057	1.6415594E-06
	26058	2.1846152E-07
	40090	2.1685556E-02
	40091	4.7501706E-03
	40092	7.2369482E-03
	40094	7.3043869E-03
	40096	1.1717381E-03
	41093	4.2334134E-04
	50112	3.2138833E-06
	50114	2.1867856E-06
	50115	1.1264842E-06
	50116	4.8173746E-05
	50117	2.5445318E-05
	50118	8.0245552E-05
	50119	2.8460301E-05
	50120	1.0794373E-04
	50122	1.5340080E-05
	50124	1.9183389E-05

4.3. TEMPERATURE

The temperatures of the materials in each region are provided in Table 5. All three codes used the ENDF/B-VII.1 [19, 20] library for the corresponding temperatures to perform the simulations documented in this report.

Table 5. Temperature of materials in each region

Regions	Temperature (K)
Fuel	900
ZIRLO clad	600
Cr coating	600
Moderator	600
Guide tube	600

4.4. SPECIFIC POWER AND DENSITY

The specific powers and densities of the fuels were obtained from CASL's Westinghouse collaborators, as listed in Table 6. These values were kept consistent between all three codes for all models.

Table 6. Specific power and density of materials in each region

Fuel	Specific Power (W/gU)	Fuel Density (g/cm^3)	U Density (g/cm^3)
UO_2	40.311	10.27825	9.05997
U_3Si_2-BeO	36.669	11.19169	10.24372
U_3Si_2-BeO-UB_2	36.666	11.19429	10.24463
$U^{15}N$-BeO	34.458	13.08105	12.16294
$U^{15}N$-BeO-UB_2	34.466	13.07850	12.16015

5. RESULTS

Various depletion methods and parameters can be defined in each code to perform depletion calculations. VERA uses a predictor-corrector approach and tracks the depletion and decay of 263 isotopes during a depletion calculation. For this benchmark exercise, Serpent calculations were executed with the predictor-corrector method and with a user-defined fission product yield cutoff of 1×10^{-6} to track isotopes of fission yields greater than this user-defined value. Shift depletion calculations were performed using the fully explicit method (set as default), which tracks all 2,200 isotopes available within the ORIGEN library in each depletable region. For the Shift calculations, the flux is renormalized at each substep based on the energy released during the depletion.

At the first time (zero burnup) for the standard UO_2 lattice, VERA agrees well with Serpent, with less than 100 pcm difference in k_{eff}, whereas Shift and VERA differ by 168 pcm. For U_3Si_2-BeO fuel, VERA and Serpent k_{eff} differ by 201 pcm, while Shift and VERA differ by 300 pcm, and for $U^{15}N$-BeO fuel, VERA and Serpent results differ by 238 pcm, whereas Shift and VERA results differ by 348 pcm. VERA and Serpent are in closer agreement for cases with UB_2 than Shift and VERA. For U_3Si_2-BeO-UB_2 fuel, VERA and Serpent k_{eff} differ by 100 pcm, while Shift and VERA differ by 317 pcm, and for $U^{15}N$-BeO-UB_2 fuel, VERA and Serpent results differ by 158 pcm, whereas Shift and VERA results differ by 340 pcm.

There are notable differences between VERA and the Monte Carlo codes, Serpent and Shift, at the first time-step. However, these differences are larger between VERA and Shift. Figure 4 shows the differences between VERA and Serpent and between VERA and Shift for each of the cases analyzed for this benchmark study. Recent changes to the thermal scattering data limit in Shift could be a root cause of differences seen between VERA and Shift, although this needs to be investigated further. To narrow in on the cause of the differences between VERA and Shift, fuel pin depletion calculations must be performed for each fuel type. This benchmark document will be revised with current findings after these pin calculations are performed. Prior depletion benchmarking efforts between VERA and Shift have shown closer agreement for UO_2 [21].

Figure 5 shows the differences between Shift and Serpent Monte Carlo codes. For non-UB_2 fuel cases, Shift and Serpent are in good agreement, especially at lower burnup. As the burnup increases, Shift has a more negative k_{eff} than Serpent, possibly due to the tracking and buildup of 2,200 nuclides that might be more significant at higher burnup. However, for fuel with UB_2, Shift and Serpent differ by ~200 pcm at zero burnup. Sections 5.1–5.5 show the k_{eff} at each time step for all the codes, and Section 5.6 shows the difference between Shift and Serpent results.

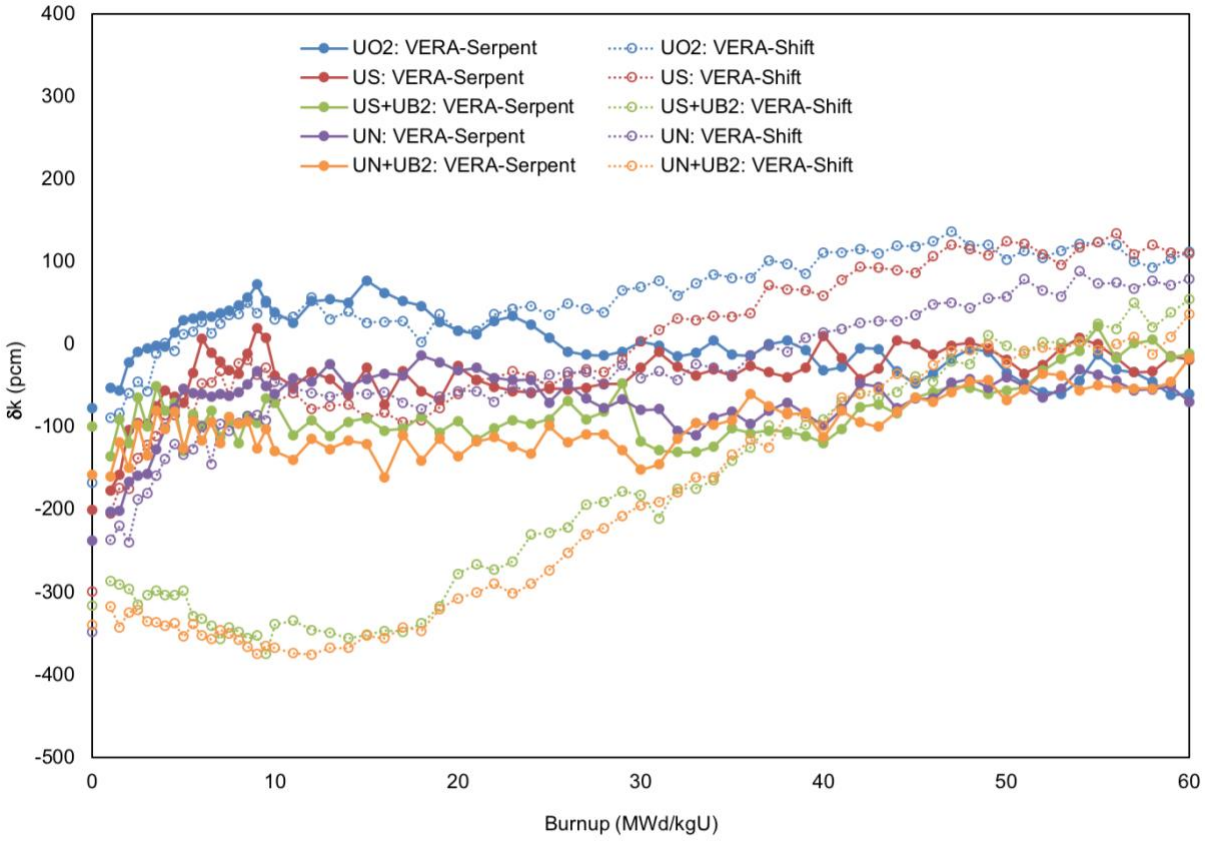

Figure 4. PWR lattice with three depletable fuel regions.

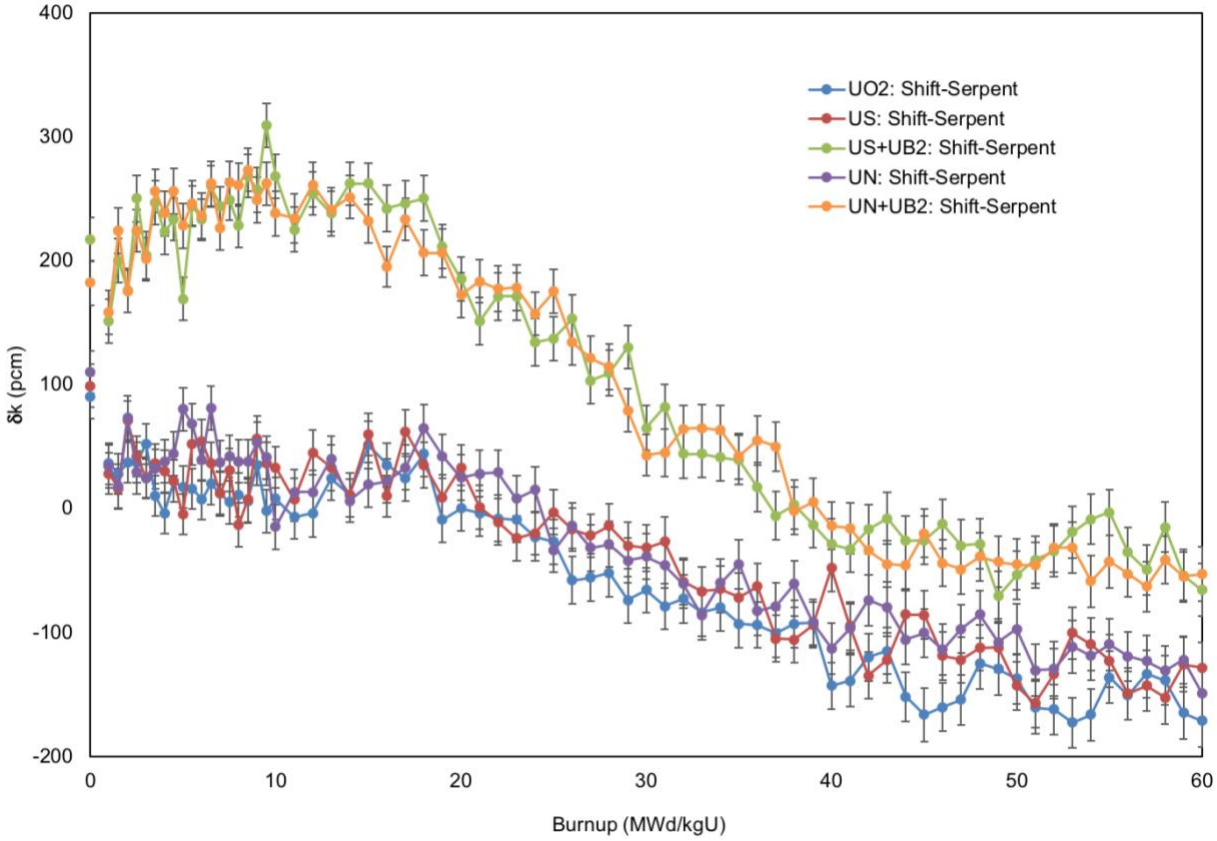

Figure 5. Differences between Shift and Serpent results.

5.1. UO_2

Table 7. Comparison of 2D 17 × 17 UO_2 results

BU (MWd/kgU)	VERA	Serpent		Shift		Difference (VERA – Serpent)		Difference (VERA – Shift)	
	k_{eff}	k_{eff}	1σ std. dev.	k_{eff}	1σ std. dev.	δk_{eff}	1σ std. dev.	δk_{eff}	1σ std. dev.
0	1.42718	1.42796	12	1.42886	13	-78	12	-168	13
1	1.36315	1.36368	12	1.36404	12	-53	12	-89	12
1.5	1.35758	1.35814	11	1.35842	12	-56	11	-84	12
2	1.35238	1.35260	11	1.35297	12	-22	11	-59	12
2.5	1.34717	1.34726	11	1.34763	12	-9	11	-46	12
3	1.34187	1.34192	11	1.34244	12	-5	11	-57	12
3.5	1.33649	1.33651	11	1.33661	12	-2	11	-12	12
4	1.33106	1.33109	12	1.33105	11	-3	12	1	11
4.5	1.32560	1.32546	12	1.32568	12	14	12	-8	12
5	1.32013	1.31984	12	1.32001	12	29	12	12	12
5.5	1.31467	1.31436	11	1.31452	12	31	11	15	12
6	1.30923	1.30889	11	1.30896	11	34	11	27	11
6.5	1.30382	1.30349	12	1.30369	12	33	12	13	12
7	1.29845	1.29808	13	1.29820	12	37	13	25	12
7.5	1.29313	1.29273	13	1.29278	12	40	13	35	12

BU (MWd/kgU)	VERA	Serpent		Shift		Difference (VERA – Serpent)		Difference (VERA – Shift)	
	k_{eff}	k_{eff}	1σ std. dev.	k_{eff}	1σ std. dev.	δk_{eff}	1σ std. dev.	δk_{eff}	1σ std. dev.
8	1.28785	1.28738	13	1.28749	12	47	13	36	12
8.5	1.28263	1.28207	13	1.28213	12	56	13	50	12
9	1.27747	1.27675	12	1.27710	11	72	12	37	11
9.5	1.27237	1.27187	13	1.27185	11	50	13	52	11
10	1.26737	1.26699	13	1.26707	11	38	13	30	11
11	1.25748	1.25722	13	1.25715	12	26	13	33	12
12	1.24780	1.24728	15	1.24724	12	52	15	56	12
13	1.23834	1.23780	13	1.23804	11	54	13	30	11
14	1.22909	1.22859	14	1.22870	11	50	14	39	11
15	1.22004	1.21927	15	1.21978	12	77	15	26	12
16	1.21117	1.21055	14	1.21090	11	62	14	27	11
17	1.20247	1.20195	14	1.20219	12	52	14	28	12
18	1.19393	1.19347	15	1.19391	11	46	15	2	11
19	1.18553	1.18526	14	1.18517	12	27	14	36	12
20	1.17731	1.17715	15	1.17715	11	16	15	16	11
21	1.16917	1.16905	15	1.16901	11	12	15	16	11
22	1.16115	1.16087	15	1.16079	11	28	15	36	11
23	1.15323	1.15289	15	1.15280	11	34	15	43	11
24	1.14540	1.14517	16	1.14494	11	23	16	46	11
25	1.13767	1.13759	15	1.13732	10	8	15	35	10
26	1.13001	1.13010	16	1.12952	10	-9	16	49	10
27	1.12244	1.12257	16	1.12201	11	-13	16	43	11
28	1.11493	1.11507	16	1.11455	11	-14	16	38	11
29	1.10750	1.10759	15	1.10685	11	-9	15	65	11
30	1.10009	1.10006	15	1.09940	10	3	15	69	10
31	1.09278	1.09280	15	1.09201	10	-2	15	77	10
32	1.08553	1.08568	16	1.08495	11	-15	16	58	11
33	1.07833	1.07844	16	1.07760	10	-11	16	73	10
34	1.07119	1.07115	16	1.07035	10	4	16	84	10
35	1.06410	1.06423	16	1.06330	11	-13	16	80	11
36	1.05706	1.05720	15	1.05626	10	-14	15	80	10
37	1.05008	1.05008	16	1.04907	11	0	16	101	11
38	1.04314	1.04310	16	1.04217	10	4	16	97	10
39	1.03625	1.03632	15	1.03540	10	-7	15	85	10
40	1.02934	1.02966	16	1.02823	10	-32	16	111	10
41	1.02255	1.02283	18	1.02144	10	-28	18	111	10
42	1.01581	1.01586	17	1.01466	9	-5	17	115	9
43	1.00912	1.00918	16	1.00803	9	-6	16	109	9
44	1.00249	1.00282	17	1.00130	10	-33	17	119	10
45	0.99591	0.99639	19	0.99473	10	-48	19	118	10
46	0.98938	0.98974	17	0.98814	10	-36	17	124	10

BU (MWd/kgU)	VERA	Serpent		Shift		Difference (VERA – Serpent)		Difference (VERA – Shift)	
	k_{eff}	k_{eff}	1σ std. dev.	k_{eff}	1σ std. dev.	δk_{eff}	1σ std. dev.	δk_{eff}	1σ std. dev.
47	0.98291	0.98309	18	0.98155	9	-18	18	136	9
48	0.97650	0.97656	18	0.97531	10	-6	18	119	10
49	0.97015	0.97024	19	0.96894	9	-9	19	121	9
50	0.96379	0.96414	18	0.96277	10	-35	18	103	10
51	0.95756	0.95804	19	0.95643	10	-48	19	113	10
52	0.95141	0.95199	18	0.95037	9	-58	18	104	9
53	0.94531	0.94591	18	0.94418	9	-60	18	113	9
54	0.93929	0.93974	19	0.93808	9	-45	19	121	9
55	0.93334	0.93347	19	0.93211	9	-13	19	123	9
56	0.92747	0.92778	17	0.92627	9	-31	17	120	9
57	0.92167	0.92201	17	0.92068	9	-34	17	99	9
58	0.91595	0.91641	18	0.91502	9	-46	18	93	9
59	0.91032	0.91094	19	0.90929	9	-62	19	103	9
60	0.90471	0.90531	19	0.90360	9	-60	19	111	9

5.2. U_3Si_2-BeO

Table 8. Comparison of 2D 17 × 17 U_3Si_2-BeO results

BU (MWd/kgU)	VERA	Serpent		Shift		Difference (VERA – Serpent)		Difference (VERA – Shift)	
	k_{eff}	k_{eff}	1σ std. dev.	k_{eff}	1σ std. dev.	δk_{eff}	1σ std. dev.	δk_{eff}	1σ std. dev.
0	1.41893	1.42094	12	1.42193	12	-201	12	-300	12
1	1.35727	1.35904	11	1.35932	12	-177	11	-205	12
1.5	1.35161	1.35319	11	1.35335	12	-158	11	-174	12
2	1.34631	1.34735	11	1.34806	11	-104	11	-175	11
2.5	1.34099	1.34195	11	1.34237	12	-96	11	-138	12
3	1.33559	1.33656	11	1.33681	12	-97	11	-122	12
3.5	1.33012	1.33087	11	1.33123	12	-75	11	-111	12
4	1.32461	1.32517	12	1.32547	12	-56	12	-86	12
4.5	1.31907	1.31971	12	1.31993	12	-64	12	-86	12
5	1.31354	1.31425	12	1.31420	11	-71	12	-66	11
5.5	1.30802	1.30837	13	1.30889	11	-35	13	-87	11
6	1.30254	1.30248	13	1.30302	12	6	13	-48	12
6.5	1.29709	1.29720	13	1.29756	11	-11	13	-47	11
7	1.29170	1.29191	12	1.29203	12	-21	12	-33	12
7.5	1.28636	1.28668	13	1.28699	11	-32	13	-63	11
8	1.28108	1.28144	13	1.28131	12	-36	13	-23	12
8.5	1.27586	1.27598	14	1.27605	12	-12	14	-19	12
9	1.27070	1.27051	15	1.27107	11	19	15	-37	11
9.5	1.26561	1.26554	13	1.26590	11	7	13	-29	11

BU (MWd/kgU)	VERA	Serpent		Shift		Difference (VERA – Serpent)		Difference (VERA – Shift)	
	k_{eff}	k_{eff}	1σ std. dev.	k_{eff}	1σ std. dev.	δk_{eff}	1σ std. dev.	δk_{eff}	1σ std. dev.
10	1.26019	1.26057	12	1.26090	12	-38	12	-71	12
11	1.25031	1.25083	13	1.25090	12	-52	13	-59	12
12	1.24065	1.24099	14	1.24144	11	-34	14	-79	11
13	1.23122	1.23164	14	1.23197	12	-42	14	-75	12
14	1.22202	1.22264	14	1.22275	11	-62	14	-73	11
15	1.21301	1.21330	13	1.21390	11	-29	13	-89	11
16	1.20419	1.20492	13	1.20502	11	-73	13	-83	11
17	1.19554	1.19587	14	1.19649	11	-33	14	-95	11
18	1.18704	1.18761	14	1.18796	12	-57	14	-92	12
19	1.17869	1.17937	14	1.17946	11	-68	14	-77	11
20	1.17068	1.17095	15	1.17128	11	-27	15	-60	11
21	1.16261	1.16304	14	1.16305	11	-43	14	-44	11
22	1.15464	1.15516	15	1.15505	11	-52	15	-41	11
23	1.14677	1.14734	15	1.14710	10	-57	15	-33	10
24	1.13900	1.13959	14	1.13939	10	-59	14	-39	10
25	1.13132	1.13186	15	1.13183	10	-54	15	-51	10
26	1.12373	1.12428	14	1.12411	10	-55	14	-38	10
27	1.11620	1.11673	14	1.11651	10	-53	14	-31	10
28	1.10876	1.10924	14	1.10910	11	-48	14	-34	11
29	1.10138	1.10186	15	1.10156	11	-48	15	-18	11
30	1.09432	1.09461	16	1.09429	10	-29	16	3	10
31	1.08709	1.08719	17	1.08692	11	-10	17	17	11
32	1.07991	1.08019	16	1.07960	10	-28	16	31	10
33	1.07279	1.07317	16	1.07250	11	-38	16	29	11
34	1.06572	1.06603	16	1.06538	10	-31	16	34	10
35	1.05871	1.05910	17	1.05838	10	-39	17	33	10
36	1.05176	1.05202	16	1.05139	10	-26	16	37	10
37	1.04486	1.04520	16	1.04415	10	-34	16	71	10
38	1.03801	1.03841	16	1.03735	10	-40	16	66	10
39	1.03121	1.03150	16	1.03056	10	-29	16	65	10
40	1.02453	1.02443	16	1.02395	10	10	16	58	10
41	1.01785	1.01802	17	1.01707	9	-17	17	78	9
42	1.01122	1.01164	16	1.01029	10	-42	16	93	10
43	1.00465	1.00495	16	1.00373	10	-30	16	92	10
44	0.99813	0.99809	17	0.99723	10	4	17	90	10
45	0.99167	0.99167	17	0.99081	10	0	17	86	10
46	0.98527	0.98540	17	0.98421	9	-13	17	106	9
47	0.97893	0.97895	16	0.97773	10	-2	16	120	10
48	0.97265	0.97263	16	0.97151	9	2	16	115	9
49	0.96644	0.96649	17	0.96537	10	-5	17	107	10
50	0.96019	0.96038	17	0.95895	10	-19	17	124	10

BU (MWd/kgU)	VERA	Serpent		Shift		Difference (VERA – Serpent)		Difference (VERA – Shift)	
	k_{eff}	k_{eff}	1σ std. dev.	k_{eff}	1σ std. dev.	δk_{eff}	1σ std. dev.	δk_{eff}	1σ std. dev.
51	0.95411	0.95447	17	0.95290	9	-36	17	121	9
52	0.94810	0.94835	18	0.94702	9	-25	18	108	9
53	0.94216	0.94221	19	0.94121	9	-5	19	96	9
54	0.93630	0.93623	19	0.93513	10	7	19	117	10
55	0.93051	0.93051	19	0.92928	10	0	19	123	10
56	0.92480	0.92496	19	0.92347	9	-16	19	133	9
57	0.91917	0.91951	18	0.91808	10	-34	18	109	10
58	0.91362	0.91395	19	0.91242	10	-33	19	120	10
59	0.90816	0.90831	20	0.90705	9	-15	20	111	9
60	0.90267	0.90286	18	0.90158	9	-19	18	109	9

5.3. U_3Si_2-BeO-UB_2

Table 9. Comparison of 2D 17 × 17 U_3Si_2-BeO-UB_2 results

BU (MWd/kgU)	VERA	Serpent		Shift		Difference (VERA – Serpent)		Difference (VERA – Shift)	
	k_{eff}	k_{eff}	1σ std. dev.	k_{eff}	1σ std. dev.	δk_{eff}	1σ std. dev.	δk_{eff}	1σ std. dev.
0	1.04609	1.04709	15	1.04926	9	-100	15	-317	9
1	1.04745	1.04881	15	1.05032	9	-136	15	-287	9
1.5	1.05964	1.06055	15	1.06255	9	-91	15	-291	9
2	1.07108	1.07228	15	1.07404	9	-120	15	-296	9
2.5	1.08163	1.08228	16	1.08478	10	-65	16	-315	10
3	1.09128	1.09228	16	1.09432	10	-100	16	-304	10
3.5	1.10008	1.10059	15	1.10306	9	-51	15	-298	9
4	1.10809	1.10890	15	1.11113	10	-81	15	-304	10
4.5	1.11538	1.11609	14	1.11842	10	-71	14	-304	10
5	1.12198	1.12328	14	1.12497	10	-130	14	-299	10
5.5	1.12795	1.12880	13	1.13124	10	-85	13	-329	10
6	1.13334	1.13433	13	1.13666	10	-99	13	-332	10
6.5	1.13817	1.13898	13	1.14158	10	-81	13	-341	10
7	1.14249	1.14362	12	1.14606	10	-113	12	-357	10
7.5	1.14633	1.14727	13	1.14976	11	-94	13	-343	11
8	1.14972	1.15092	14	1.15320	10	-120	14	-348	10
8.5	1.15268	1.15356	14	1.15624	10	-88	14	-356	10
9	1.15524	1.15620	15	1.15877	10	-96	15	-353	10
9.5	1.15743	1.15809	14	1.16118	10	-66	14	-375	10
10	1.15927	1.15998	14	1.16266	11	-71	14	-339	11
11	1.16196	1.16306	15	1.16531	10	-110	15	-335	10
12	1.16349	1.16441	14	1.16695	10	-92	14	-346	10
13	1.16399	1.16510	15	1.16748	10	-111	15	-349	10
14	1.16356	1.16450	14	1.16712	10	-94	14	-356	10

BU (MWd/kgU)	VERA	Serpent		Shift		Difference (VERA – Serpent)		Difference (VERA – Shift)	
	k_{eff}	k_{eff}	1σ std. dev.	k_{eff}	1σ std. dev.	δk_{eff}	1σ std. dev.	δk_{eff}	1σ std. dev.
15	1.16231	1.16321	13	1.16583	11	-90	13	-352	11
16	1.16034	1.16139	15	1.16381	11	-105	15	-347	11
17	1.15773	1.15875	15	1.16121	11	-102	15	-348	11
18	1.15456	1.15544	15	1.15794	11	-88	15	-338	11
19	1.15090	1.15197	14	1.15408	11	-107	14	-318	11
20	1.14684	1.14777	14	1.14962	11	-93	14	-278	11
21	1.14238	1.14354	16	1.14505	10	-116	16	-267	10
22	1.13758	1.13860	16	1.14031	10	-102	16	-273	10
23	1.13251	1.13343	16	1.13514	11	-92	16	-263	11
24	1.12718	1.12815	16	1.12949	11	-97	16	-231	11
25	1.12165	1.12256	14	1.12393	11	-91	14	-228	11
26	1.11593	1.11662	16	1.11815	11	-69	16	-222	11
27	1.11006	1.11097	15	1.11200	11	-91	15	-194	11
28	1.10406	1.10488	15	1.10597	11	-82	15	-191	11
29	1.09795	1.09843	14	1.09973	10	-48	14	-178	10
30	1.09131	1.09249	15	1.09314	11	-118	15	-183	11
31	1.08502	1.08631	15	1.08713	10	-129	15	-211	10
32	1.07867	1.07998	16	1.08042	11	-131	16	-175	11
33	1.07228	1.07359	16	1.07403	10	-131	16	-175	10
34	1.06586	1.06710	16	1.06751	10	-124	16	-165	10
35	1.05942	1.06044	17	1.06083	10	-102	17	-141	10
36	1.05296	1.05404	17	1.05421	10	-108	17	-125	10
37	1.04649	1.04754	17	1.04748	10	-105	17	-99	10
38	1.04003	1.04109	17	1.04112	10	-106	17	-109	10
39	1.03358	1.03469	16	1.03456	10	-111	16	-98	10
40	1.02706	1.02826	18	1.02797	10	-120	18	-91	10
41	1.02065	1.02168	16	1.02135	10	-103	16	-70	10
42	1.01426	1.01502	17	1.01485	10	-76	17	-59	10
43	1.00789	1.00862	18	1.00854	10	-73	18	-65	10
44	1.00157	1.00241	17	1.00215	10	-84	17	-58	10
45	0.99528	0.99593	17	0.99567	10	-65	17	-39	10
46	0.98903	0.98961	17	0.98948	10	-58	17	-45	10
47	0.98283	0.98334	18	0.98304	10	-51	18	-21	10
48	0.97667	0.97720	18	0.97692	9	-53	18	-24	9
49	0.97057	0.97117	18	0.97046	9	-60	18	11	9
50	0.96459	0.96515	17	0.96461	10	-56	17	-2	10
51	0.95861	0.95914	17	0.95873	9	-53	17	-12	9
52	0.95269	0.95301	18	0.95267	10	-32	18	3	10
53	0.94682	0.94700	19	0.94681	9	-18	19	1	9
54	0.94103	0.94111	18	0.94102	10	-8	18	1	10
55	0.93530	0.93509	16	0.93506	9	21	16	24	9

BU (MWd/kgU)	VERA	Serpent		Shift		Difference (VERA – Serpent)		Difference (VERA – Shift)	
	k_{eff}	k_{eff}	1σ std. dev.	k_{eff}	1σ std. dev.	δk_{eff}	1σ std. dev.	δk_{eff}	1σ std. dev.
56	0.92964	0.92981	18	0.92946	9	-17	18	18	9
57	0.92405	0.92404	18	0.92355	9	1	18	51	9
58	0.91854	0.91849	18	0.91834	9	5	18	20	9
59	0.91310	0.91326	19	0.91272	9	-16	19	38	9
60	0.90776	0.90788	19	0.90722	10	-12	19	54	10

5.4. $U^{15}N$-BeO

Table 10. Comparison of 2D 17 × 17 $U^{15}N$-BeO results

BU (MWd/kgU)	VERA	Serpent		Shift		Difference (VERA – Serpent)		Difference (VERA – Shift)	
	k_{eff}	k_{eff}	1σ std. dev.	k_{eff}	1σ std. dev.	δk_{eff}	1σ std. dev.	δk_{eff}	1σ std. dev.
0	1.42587	1.42825	12	1.42935	12	-238	12	-348	12
1	1.36466	1.36669	12	1.36703	13	-203	12	-237	13
1.5	1.35900	1.36102	12	1.36120	13	-202	12	-220	13
2	1.35368	1.35535	13	1.35608	13	-167	13	-240	13
2.5	1.34834	1.34993	12	1.35022	12	-159	12	-188	12
3	1.34293	1.34450	11	1.34474	12	-157	11	-181	12
3.5	1.33745	1.33872	11	1.33904	12	-127	11	-159	12
4	1.33193	1.33294	12	1.33332	12	-101	12	-139	12
4.5	1.32639	1.32716	13	1.32760	12	-77	13	-121	12
5	1.32085	1.32139	13	1.32219	12	-54	13	-134	12
5.5	1.31533	1.31592	12	1.31660	12	-59	12	-127	12
6	1.30984	1.31045	12	1.31084	11	-61	12	-100	11
6.5	1.30439	1.30503	13	1.30584	12	-64	13	-145	12
7	1.29900	1.29960	13	1.29997	12	-60	13	-97	12
7.5	1.29365	1.29428	13	1.29470	11	-63	13	-105	11
8	1.28837	1.28895	13	1.28933	12	-58	13	-96	12
8.5	1.28315	1.28364	13	1.28402	12	-49	13	-87	12
9	1.27799	1.27832	12	1.27885	12	-33	12	-86	12
9.5	1.27290	1.27341	13	1.27382	11	-51	13	-92	11
10	1.26788	1.26849	14	1.26834	11	-61	14	-46	11
11	1.25802	1.25843	14	1.25856	12	-41	14	-54	12
12	1.24840	1.24886	13	1.24899	12	-46	13	-59	12
13	1.23900	1.23924	14	1.23964	11	-24	14	-64	11
14	1.22982	1.23034	13	1.23040	12	-52	13	-58	12
15	1.22084	1.22126	14	1.22145	12	-42	14	-61	12
16	1.21204	1.21240	14	1.21262	11	-36	14	-58	11
17	1.20342	1.20380	14	1.20413	12	-38	14	-71	12
18	1.19494	1.19508	15	1.19573	11	-14	15	-79	11

BU (MWd/kgU)	VERA	Serpent		Shift		Difference (VERA – Serpent)		Difference (VERA – Shift)	
	k_{eff}	k_{eff}	1σ std. dev.	k_{eff}	1σ std. dev.	δk_{eff}	1σ std. dev.	δk_{eff}	1σ std. dev.
19	1.18661	1.18683	14	1.18725	11	-22	14	-64	11
20	1.17823	1.17855	15	1.17880	11	-32	15	-57	11
21	1.17014	1.17043	15	1.17071	11	-29	15	-57	11
22	1.16216	1.16257	15	1.16286	10	-41	15	-70	10
23	1.15427	1.15471	15	1.15479	10	-44	15	-52	10
24	1.14648	1.14691	15	1.14706	11	-43	15	-58	11
25	1.13878	1.13949	14	1.13915	11	-71	14	-37	11
26	1.13115	1.13163	15	1.13149	11	-48	15	-34	11
27	1.12360	1.12426	15	1.12394	11	-66	15	-34	11
28	1.11612	1.11690	15	1.11661	11	-78	15	-49	11
29	1.10871	1.10938	15	1.10896	11	-67	15	-25	11
30	1.10101	1.10181	15	1.10142	11	-80	15	-41	11
31	1.09370	1.09449	14	1.09403	11	-79	14	-33	11
32	1.08645	1.08750	16	1.08689	11	-105	16	-44	11
33	1.07926	1.08036	17	1.07950	11	-110	17	-24	11
34	1.07212	1.07301	16	1.07241	10	-89	16	-29	10
35	1.06504	1.06586	17	1.06541	10	-82	17	-37	10
36	1.05801	1.05898	17	1.05815	10	-97	17	-14	10
37	1.05102	1.05183	16	1.05104	10	-81	16	-2	10
38	1.04409	1.04480	16	1.04419	10	-71	16	-10	10
39	1.03722	1.03806	16	1.03714	10	-84	16	8	10
40	1.03053	1.03152	18	1.03039	10	-99	18	14	10
41	1.02376	1.02455	17	1.02358	10	-79	17	18	10
42	1.01705	1.01753	18	1.01679	10	-48	18	26	10
43	1.01038	1.01090	18	1.01010	10	-52	18	28	10
44	1.00378	1.00456	17	1.00350	10	-78	17	28	10
45	0.99723	0.99789	17	0.99688	10	-66	17	35	10
46	0.99073	0.99139	18	0.99025	10	-66	18	48	10
47	0.98430	0.98477	17	0.98380	10	-47	17	50	10
48	0.97793	0.97835	16	0.97750	10	-42	16	43	10
49	0.97162	0.97215	16	0.97107	10	-53	16	55	10
50	0.96549	0.96589	18	0.96492	9	-40	18	57	9
51	0.95932	0.95984	19	0.95853	9	-52	19	79	9
52	0.95322	0.95387	20	0.95258	10	-65	20	64	10
53	0.94719	0.94773	19	0.94662	9	-54	19	57	9
54	0.94123	0.94154	17	0.94035	10	-31	17	88	10
55	0.93535	0.93572	19	0.93462	9	-37	19	73	9
56	0.92954	0.92999	18	0.92880	9	-45	18	74	9
57	0.92382	0.92438	19	0.92315	9	-56	19	67	9
58	0.91818	0.91873	18	0.91742	9	-55	18	76	9
59	0.91262	0.91313	17	0.91191	9	-51	17	71	9

BU (MWd/kgU)	VERA	Serpent		Shift		Difference (VERA – Serpent)		Difference (VERA – Shift)	
	k_{eff}	k_{eff}	1σ std. dev.	k_{eff}	1σ std. dev.	δk_{eff}	1σ std. dev.	δk_{eff}	1σ std. dev.
60	0.90714	0.90784	18	0.90635	9	-70	18	79	9

5.5. $U^{15}N$-BeO-UB_2

Table 11. Comparison of 2D 17 × 17 $U^{15}N$-BeO-UB_2 results

BU (MWd/kgU)	VERA	Serpent		Shift		Difference (VERA – Serpent)		Difference (VERA – Shift)	
	k_{eff}	k_{eff}	1σ std. dev.	k_{eff}	1σ std. dev.	δk_{eff}	1σ std. dev.	δk_{eff}	1σ std. dev.
0	1.07956	1.08114	15	1.08296	10	-158	15	-340	10
1	1.07783	1.07943	15	1.08101	9	-160	15	-318	9
1.5	1.08908	1.09027	15	1.09251	10	-119	15	-343	10
2	1.09961	1.10111	14	1.10286	9	-150	14	-325	9
2.5	1.10926	1.11024	14	1.11248	9	-98	14	-322	9
3	1.11803	1.11938	14	1.12139	10	-135	14	-336	10
3.5	1.12597	1.12678	14	1.12934	10	-81	14	-337	10
4	1.13314	1.13417	15	1.13655	10	-103	15	-341	10
4.5	1.13960	1.14042	15	1.14298	10	-82	15	-338	10
5	1.14541	1.14667	15	1.14895	10	-126	15	-354	10
5.5	1.15061	1.15154	15	1.15400	10	-93	15	-339	10
6	1.15524	1.15641	15	1.15877	10	-117	15	-353	10
6.5	1.15935	1.16030	15	1.16292	10	-95	15	-357	10
7	1.16298	1.16418	14	1.16644	11	-120	14	-346	11
7.5	1.16614	1.16702	14	1.16965	10	-88	14	-351	10
8	1.16888	1.16985	14	1.17246	10	-97	14	-358	10
8.5	1.17123	1.17216	14	1.17489	10	-93	14	-366	10
9	1.17320	1.17446	15	1.17695	11	-126	15	-375	11
9.5	1.17482	1.17585	14	1.17847	10	-103	14	-365	10
10	1.17594	1.17724	14	1.17962	11	-130	14	-368	11
11	1.17759	1.17899	16	1.18133	11	-140	16	-374	11
12	1.17818	1.17933	15	1.18194	10	-115	15	-376	10
13	1.17782	1.17909	14	1.18150	10	-127	14	-368	10
14	1.17660	1.17777	14	1.18028	10	-117	14	-368	10
15	1.17465	1.17586	14	1.17818	11	-121	14	-353	11
16	1.17204	1.17365	13	1.17560	10	-161	13	-356	10
17	1.16886	1.16996	13	1.17229	11	-110	13	-343	11
18	1.16517	1.16658	15	1.16864	11	-141	15	-347	11
19	1.16104	1.16219	16	1.16425	11	-115	16	-321	11
20	1.15653	1.15789	14	1.15961	11	-136	14	-308	11
21	1.15168	1.15286	14	1.15469	10	-118	14	-301	10
22	1.14655	1.14768	15	1.14945	11	-113	15	-290	11

BU (MWd/kgU)	VERA	Serpent		Shift		Difference (VERA – Serpent)		Difference (VERA – Shift)	
	k_{eff}	k_{eff}	1σ std. dev.	k_{eff}	1σ std. dev.	δk_{eff}	1σ std. dev.	δk_{eff}	1σ std. dev.
23	1.14116	1.14240	15	1.14418	10	-124	15	-302	10
24	1.13555	1.13688	14	1.13845	11	-133	14	-290	11
25	1.12975	1.13074	14	1.13249	11	-99	14	-274	11
26	1.12380	1.12499	15	1.12633	11	-119	15	-253	11
27	1.11771	1.11880	15	1.12001	10	-109	15	-230	10
28	1.11151	1.11260	15	1.11374	11	-109	15	-223	11
29	1.10522	1.10651	14	1.10730	10	-129	14	-208	10
30	1.09881	1.10033	13	1.10076	11	-152	13	-195	11
31	1.09237	1.09383	16	1.09428	10	-146	16	-191	10
32	1.08589	1.08704	16	1.08768	11	-115	16	-179	11
33	1.07938	1.08034	16	1.08099	10	-96	16	-161	10
34	1.07283	1.07381	17	1.07444	11	-98	17	-161	11
35	1.06627	1.06719	15	1.06761	11	-92	15	-134	11
36	1.05970	1.06031	17	1.06086	10	-61	17	-116	10
37	1.05312	1.05387	17	1.05437	10	-75	17	-125	10
38	1.04656	1.04741	16	1.04739	11	-85	16	-83	11
39	1.04000	1.04083	17	1.04088	10	-83	17	-88	10
40	1.03334	1.03447	16	1.03433	10	-113	16	-99	10
41	1.02682	1.02763	18	1.02747	10	-81	18	-65	10
42	1.02033	1.02128	17	1.02094	10	-95	17	-61	10
43	1.01387	1.01487	16	1.01442	10	-100	16	-55	10
44	1.00744	1.00826	16	1.00780	10	-82	16	-36	10
45	1.00105	1.00170	17	1.00150	9	-65	17	-45	9
46	0.99470	0.99540	16	0.99496	10	-70	16	-26	10
47	0.98840	0.98898	17	0.98849	10	-58	17	-9	10
48	0.98215	0.98261	17	0.98222	10	-46	17	-7	10
49	0.97594	0.97638	18	0.97595	9	-44	18	-1	9
50	0.96959	0.97027	18	0.96982	9	-68	18	-23	9
51	0.96350	0.96405	16	0.96359	9	-55	16	-9	9
52	0.95747	0.95783	17	0.95751	10	-36	17	-4	10
53	0.95150	0.95188	18	0.95157	10	-38	18	-6	10
54	0.94559	0.94615	19	0.94556	9	-56	19	3	9
55	0.93976	0.94026	19	0.93983	9	-50	19	-7	9
56	0.93399	0.93452	17	0.93399	8	-53	17	0	8
57	0.92830	0.92884	18	0.92821	9	-54	18	9	9
58	0.92269	0.92323	17	0.92281	9	-54	17	-12	9
59	0.91715	0.91761	17	0.91706	9	-46	17	9	9
60	0.91170	0.91187	20	0.91134	9	-17	20	36	9

5.6. DIFFERENCE BETWEEN SHIFT AND SERPENT RESULTS

Table 12. Comparison of results from Shift and Serpent Monte Carlo codes

BU (MWd/kgU)	UO_2		U_3Si_2-BeO		U_3Si_2-BeO-UB_2		$U^{15}N$-BeO		$U^{15}N$-BeO-UB_2	
	k_{eff}	1σ stdev.	k_{eff}	1σ stdev.	k_{eff}	1σ stdev.	k_{eff}	1σ stdev.	k_{eff}	1σ stdev.
0.0	90	17	99	17	217	18	110	17	182	18
1.0	36	17	28	17	151	18	34	17	158	18
1.5	28	16	16	16	200	18	18	18	224	18
2.0	37	16	71	16	176	18	73	18	175	17
2.5	37	16	42	16	250	19	29	17	224	17
3.0	52	16	25	16	204	19	24	16	201	17
3.5	10	16	36	16	247	18	32	16	256	17
4.0	-4	16	30	17	223	18	38	17	238	18
4.5	22	17	22	17	233	17	44	18	256	18
5.0	17	17	-5	16	169	17	80	18	228	18
5.5	16	16	52	17	244	16	68	17	246	18
6.0	7	16	54	18	233	17	39	17	236	18
6.5	20	17	36	17	260	17	81	18	262	18
7.0	12	18	12	17	244	16	37	18	226	18
7.5	5	17	31	17	249	17	42	17	263	17
8.0	11	18	-13	18	228	17	38	18	261	17
8.5	6	18	7	18	268	17	38	17	273	17
9.0	35	16	56	18	257	18	53	17	249	18
9.5	-2	17	36	17	309	17	41	17	262	17
10.0	8	17	33	17	268	18	-15	18	238	18
11.0	-7	18	7	18	225	18	13	18	234	20
12.0	-4	19	45	18	254	17	13	18	261	18
13.0	24	17	33	18	238	18	40	18	241	17
14.0	11	18	11	18	262	17	6	17	251	17
15.0	51	19	60	17	262	17	19	18	232	18
16.0	35	18	10	17	242	19	22	18	195	16
17.0	24	18	62	18	246	19	33	18	233	17
18.0	44	19	35	18	250	19	65	19	206	18
19.0	-9	18	9	18	211	18	42	18	206	20
20.0	0	18	33	18	185	18	25	18	172	18
21.0	-4	19	1	18	151	19	28	19	183	17
22.0	-8	19	-11	19	171	19	29	18	177	18
23.0	-9	18	-24	18	171	19	8	18	178	18
24.0	-23	19	-20	17	134	19	15	18	157	18
25.0	-27	18	-3	18	137	18	-34	18	175	18
26.0	-58	19	-17	17	153	19	-14	18	134	18
27.0	-56	19	-22	17	103	19	-32	19	121	18
28.0	-52	19	-14	18	109	18	-29	18	114	18

BU (MWd/kgU)	UO_2		U_3Si_2-BeO		U_3Si_2-BeO-UB_2		$U^{15}N$-BeO		$U^{15}N$-BeO-UB_2	
	k_{eff}	1σ stdev.	k_{eff}	1σ stdev.	k_{eff}	1σ stdev.	k_{eff}	1σ stdev.	k_{eff}	1σ stdev.
29.0	-74	19	-30	19	130	17	-42	18	79	17
30.0	-66	18	-32	19	65	18	-39	18	43	17
31.0	-79	18	-27	20	82	18	-46	18	45	19
32.0	-73	19	-59	19	44	19	-61	19	64	19
33.0	-84	19	-67	19	44	19	-86	20	65	19
34.0	-80	19	-65	19	41	19	-60	19	63	20
35.0	-93	19	-72	20	39	20	-45	20	42	18
36.0	-94	18	-63	19	17	20	-83	20	55	20
37.0	-101	19	-105	19	-6	20	-79	19	50	20
38.0	-93	19	-106	19	3	20	-61	19	-2	19
39.0	-92	18	-94	19	-13	19	-92	19	5	20
40.0	-143	19	-48	19	-29	21	-113	21	-14	19
41.0	-139	21	-95	19	-33	19	-97	20	-16	20
42.0	-120	19	-135	19	-17	20	-74	20	-34	20
43.0	-115	19	-122	19	-8	21	-80	21	-45	19
44.0	-152	20	-86	20	-26	20	-106	20	-46	19
45.0	-166	22	-86	20	-26	20	-101	20	-20	19
46.0	-160	20	-119	19	-13	20	-114	20	-44	19
47.0	-154	20	-122	19	-30	21	-97	20	-49	20
48.0	-125	20	-113	18	-28	20	-86	19	-39	20
49.0	-130	21	-112	20	-71	20	-108	19	-43	20
50.0	-138	20	-143	20	-54	20	-97	20	-45	20
51.0	-161	21	-157	19	-41	19	-131	21	-46	18
52.0	-162	20	-133	20	-35	20	-129	22	-32	20
53.0	-173	20	-101	21	-19	21	-111	21	-31	20
54.0	-167	21	-110	21	-9	20	-119	20	-59	21
55.0	-136	21	-123	21	-3	19	-110	21	-43	21
56.0	-151	19	-149	21	-35	20	-119	20	-53	19
57.0	-133	19	-143	20	-50	20	-123	21	-63	20
58.0	-139	20	-153	21	-15	20	-131	20	-42	19
59.0	-165	21	-126	22	-54	21	-122	19	-55	19
60.0	-171	21	-128	20	-66	21	-149	20	-53	22

6. SUMMARY AND FUTURE WORK

DOE-NE's cooperation with the NRC to facilitate the licensing of ATF concepts and to accelerate the analysis of various design concepts has led to an effort within CASL to identify any M&S gaps of ATF concepts. This benchmark effort sought to show differences between VERA, Shift, and Serpent in the k_{eff} at various burnups during a depletion calculation. CASL's Westinghouse collaborators identified the following ATF concepts for PWRs as benchmark problems for M&S tools:

- U_3Si_2-BeO fuel and chromium coated ZIRLO cladding
- U_3Si_2-BeO-UB_2 and chromium coated ZIRLO cladding
- $U^{15}N$-BeO and chromium coated ZIRLO cladding
- $U^{15}N$-BeO-UB_2 and chromium coated ZIRLO cladding

The depletion parameters and flags used to run these models differ between all three codes. There were differences seen in k_{eff} between VERA, Shift, and Serpent, especially between VERA and Shift at the first time-step for ATF concepts. The differences identified in this document must be investigated further by modeling single fuel pin depletion to compare the isotopic evolution of the fuel during a depletion calculation. Prior depletion benchmarking efforts between VERA and Shift have shown closer agreement for UO_2, so recent changes to the code and the data must be examined to identify the cause of these differences.

ACKNOWLEDGMENTS

The VERA and Shift cases used resources of the Compute and Data Environment for Science (CADES) at ORNL, which is supported by DOE's Office of Science under Contract No. DE-AC05-00OR22725.

The authors would like to acknowledge the support received from the MPACT and Shift development teams for this work.

REFERENCES

1. United States Department of Energy, "Development of Light Water Reactor Fuels with Enhanced Accident Tolerance," Report to United States Congress (2015).
2. T. Miller, "Advanced Modeling and Simulation, Accident Tolerant Fuel Application," US Department of Energy Office of Nuclear Energy (2018). Presentation available through the NRC website at https://www.nrc.gov/reading-rm/doc-collections/commission/slides/2018/20180412/miller-20180412.pdf. Webpage visited in April 2019.
3. The Consortium for Advanced Simulation of Light Water Reactors, <https://www.casl.gov>. Webpage visited in April 2019.
4. J. A. Turner et al., "The Virtual Environment for Reactor Applications (VERA): Design and architecture," *Journal of Computational Physics*, **326**, 544 (2016).
5. J. Leppänen, M. Pusa, T. Viitanen, V. Valtavirta, and T. Kaltiaisenaho, "The Serpent Monte Carlo code: Status, development and applications in 2013," *Annals of Nuclear Energy*, **82** pp 142–150 (2015).

6. T. M. Pandya, S. R. Johnson, T. M. Evans, G. G. Davidson, S. P. Hamilton, and A. T. Godfrey, "Capabilities, Implementation, and Benchmarking of Shift, a Massively Parallel Monte Carlo Radiation Transport Code," *Journal of Computational Physics*, **308**, 239 (2016).
7. US Department of Energy Office of Nuclear Energy, "DOE Awards $111 Million to U.S. Vendors to Develop Accident Tolerant Nuclear Fuels," <https://www.energy.gov/ne/articles/doe-awards-111-million-us-vendors-develop-accident-tolerant-nuclear-fuels>. Webpage visited in April 2019.
8. NEI, "Accident Tolerant Fuel," <https://www.nei.org/advocacy/make-regulations-smarter/accident-tolerant-fuel>. Webpage visited in April 2019.
9. Westinghouse Nuclear, "Accident-tolerant Fuel," <http://www.westinghousenuclear.com/Portals/0/Technovation%20Stuff/Accident%20Tolerant%20Fuel%20Brochure%20.pdf>. Webpage visited in April 2019.
10. J. P. Mazzoccoli, J. Choi and P. Xu, "Progress on the Westinghouse Accident Tolerant Fuel Programme," Accident Tolerant Fuel Concepts for Light Water Reactors - Proceedings of a technical meeting held at ORNL, IAEA-TECDOC-1797 (2014).
11. B. Collins et al., "Stability and Accuracy of 3D Neutron Transport Simulations Using the 2D/1D Method in MPACT," *Journal of Computational Physics*, **326**, 612 (2016).
12. R. K. Salko and M. N. Avramova, "CTF Theory Manual," The Pennsylvania State University (2012).
13. W. Wieselquist, "The SCALE 6.2 ORIGEN API for High Performance Depletion," *Proc. M&C and SNA 2014*, Nashville, TN, USA (2015).
14. B. T. Rearden and M. A. Jessee, Eds., SCALE Code System, ORNL/TM-2005/39, Version 6.2.3, Oak Ridge National Laboratory, Oak Ridge, Tennessee (2018). Available from the Radiation Safety Information Computational Center as CCC-834.
15. MCNP Team, *MCNP6 Users Manual – Code Version 6.1.1beta*, LA-CP-14-00745, Los Alamos National Laboratory (2014).
16. "Serpent: a Continuous-energy Monte Carlo Reactor Physics Burnup Calculation Code," <http://montecarlo.vtt.fi>. Webpage visited in April 2019.
17. A. T. Godfrey, "VERA Core Physics Benchmark Progression Problem Specifications," Consortium for Advanced Simulation of Light Water Reactors, CASL-U-2012-0131-004 (2014).
18. F. Franceschini, *ATF CASL Fuel Specifications*, obtained in January, 2019.
19. M. B. Chadwick et al., "ENDF/B-VII.1 Nuclear Data for Science and Technology: Cross Sections, Covariances, Fission Product Yields and Decay Data," *Nuclear Data Sheets*, **112** (12), p. 2887–2996 (2011).
20. K. S. Kim et al., "Verification and validation of the ENDF/B-VII.1 v4.3m1 MPACT 51-group cross section library," Consortium for Advanced Simulation of Light Water Reactors, CASL-U-2018-1528-000, Oak Ridge National Laboratory (2018).
21. G. G. Davidson, T. M. Pandya, S. R. Johnson, T. M. Evans, A. E. Isotalo, C. A. Gentry, and W. A. Wieselquist, "Nuclide Depletion Capabilities in the Shift Monte Carlo Code," *Annals of Nuclear Energy*, **114**, pp. 259–276 (2018).